

Design of the Shaped Offset Cassegrain Antenna System Combined with Corrugated Conical Feed Horn

Doo-Yeong Yang^{*}
(梁斗榮^{*})

Abstract

In this paper, the design for the shaped offset cassegrain antenna system combined with corrugated feed horn is presented. First, spherical-mode wave theory is applied to the corrugated conical horn and its radiation patterns are investigated. Using the radiation patterns, design data of the corrugated conical horn are obtained by efficiency investigation of horn antenna. When the investigation is completed, the flare angle and length of the corrugated conical horn is determined. Next, the main and sub-reflector is designed using Snell's law and the conservation principle of energy. Then the uniform direction and energy density of the traveling wave at the aperture of the main-reflector is obtained. The maximum size of the main-reflector is determined by investigation of the illumination and spillover efficiency. Finally, the curvature of the main-reflector is modified to satisfy the condition of the uniform phase. From the calculated efficiencies, the designed size of the main-reflector and sub-reflector, system gain of the shaped offset cassegrain antenna has been obtained 40.5dB in Ka-band frequency. It has better characteristics than the result of SABOR with 39dB gain.

I. Introduction

The cassegrain antenna system is mainly used in antennae for satellite communication earth stations. This system consists of a main and a sub-reflector with a corrugated feed horn. The corrugated feed horn has a symmetrical radiation pattern and an especially large ratio of co-polarization to cross-polarization. This unique characteristic results in wide usage in antennae of dual polarized feed systems. There are two methods of corrugated conical horn analysis: cylindrical-mode analysis and spherical-mode analysis. When the flare

angle is sufficiently small, the cylindrical-mode analysis is applied to the corrugated conical horn because it enables better maintenance of the feeding electric-field at the horn. When the flare angle is larger than 10 degrees, the spherical-mode analysis is used for obtaining accurate result[1]. Using the spherical-mode analysis, Mantzer[2] presented the method for determining the slot width and tooth thickness, and Jansen[3] demonstrated that the slot depth was quarter wavelength.

The classical cassegrain antenna system simply consists of a parabolic contour for the main-reflector and a hyperbolic contour for the sub-reflector. This antenna has some characteristic of low efficiency defects and large blocking because of the non-uniform phase at the aperture of the main-reflector[4],[5]. In order to

* 濟州大學校 通信工學科

(Dept. of Telecom. Eng., Cheju Nat'l Univ.)

接受日: 1999年2月25日, 修正完了日: 1999年5月20日

reduce these defects, the spillover and the illumination efficiency concerning the radiation patterns of the corrugated conical horn have to be closely investigated. In addition, the curvature of the main-reflector must be modified to have uniform phase. Compared to the classical cassegrain antenna, the shaped offset cassegrain antenna has favorable efficiency and high gain.

II. Propagation characteristics of corrugated conical feed horn

Fig. 1 illustrates a section through a conical horn with corrugated walls and the spherical coordinate system for horn analysis. If the flare angle(θ_1) of the horn is sufficiently small, an analysis of the mode in the horn can be undertaken using cylindrical-mode function. However, when the flare angle exceeds about 10 degrees, it is necessary to utilize spherical-mode function if an accurate analysis is required. When $\theta < \theta_1$, the inner field of the horn is the hybrid-mode which has TE and TM mode simultaneously[6].

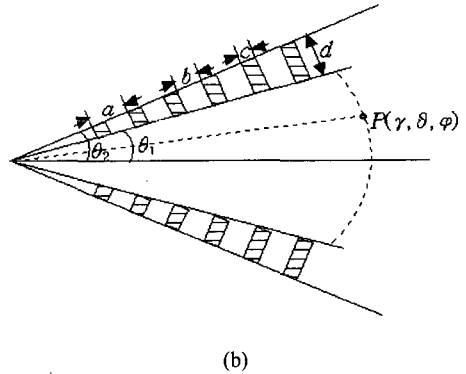
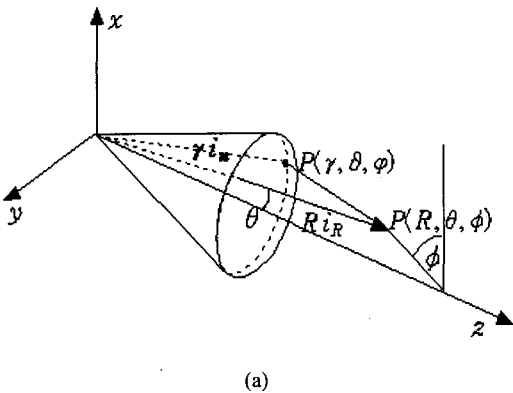


Fig.1 Geometry of the corrugated conical horn
a) spherical coordinates, b) cross section

An electromagnetic field in terms of spherical wave functions can be constructed as a superposition of its TM and TE mode in the feed horn. The modal field in the horn is derived from the electric potential and magnetic potential.

$$\begin{aligned}
 E_r &= A\eta_0 \frac{\nu(\nu+1)}{jkr^2} \hat{H}_\nu P_\nu^m \\
 H_r &= -A\bar{\Lambda} \frac{\nu(\nu+1)}{kr^2} \hat{H}_\nu P_\nu^m \\
 E_\theta &= -\eta_0 A \left(\frac{-m\bar{\Lambda}}{r\sin\theta} \hat{H}_\nu P_\nu^m + \frac{j}{r} \hat{H}_\nu' \frac{dP_\nu^m}{d\theta} \right) \\
 E_\phi &= \eta_0 A \left(\frac{-j\bar{\Lambda}}{r} \hat{H}_\nu \frac{dP_\nu^m}{d\theta} + \frac{m}{r\sin\theta} \hat{H}_\nu' P_\nu^m \right) \\
 H_\theta &= A \left(\frac{jm}{r\sin\theta} \hat{H}_\nu P_\nu^m - \bar{\Lambda} \frac{\hat{H}_\nu'}{r} \frac{dP_\nu^m}{d\theta} \right) \\
 H_\phi &= -A \left(\frac{\hat{H}_\nu}{r} \frac{dP_\nu^m}{d\theta} + j \frac{\bar{\Lambda}m}{r\sin\theta} \hat{H}_\nu' P_\nu^m \right)
 \end{aligned} \tag{1}$$

w h e r e
 $\hat{H}_\nu = \hat{H}_\nu^{(2)}(kr) = k r \cdot h_\nu^{(2)}(kr)$, $P_\nu^m = P_\nu^m(\cos\theta)$
 and $h_\nu^{(2)}(kr)$ is a spherical Hankel function of the 2nd kind of ν order, and P_ν^m is an associated Legendre function of the 1st kind of ν order. A and η_0 are amplitude coefficient of electric field and wave

impedance of free space. The coefficient \overline{A} depends on the boundary conditions. In all of the field components in spherical coordinates, the factor $e^{jm\phi}$ omitted.

For $\theta < \theta_1$ region with hybrid mode, applying boundary condition at $\theta = \theta_1$ slot's admittance is obtained.

$$Y = \left. \frac{H_\phi}{E_r} \right|_{\theta=\theta_1} = \frac{-jkr y_0}{\nu(\nu+1)} \left(p_\nu^m(\theta_1) + \frac{j\overline{A} m h_{(2)}}{\sin \theta_1} \right)$$

where

$$p_\nu^m(\theta) = \frac{dP_\nu^m(\cos \theta)}{P_\nu^m(\cos \theta) d\theta}, \quad h_\nu = h_\nu(kr) = \frac{\widehat{H}_\nu'(kr)}{\widehat{H}_\nu(kr)}$$

Equation (2) becomes

$$p_\nu^m(\theta_1) \{ \overline{Y} + p_\nu^m(\theta_1) \} = \frac{-m^2}{\sin^2 \theta_1} (h_\nu)^2 \quad (3)$$

$$\overline{Y} = \frac{-jY}{y_0} \frac{\nu(\nu+1)}{kr}, \quad y_0 = (\epsilon_0 / \mu_0)^{1/2}$$

For $\theta_1 < \theta < \theta_2$ region with TM mode, admittance for slots formed on spherical surfaces after applying boundary condition at $\theta = \theta_2$ is expressed as follows:

$$Y = \left. \frac{H_\phi}{E_r} \right|_{\theta=\theta_2} = \frac{-jy_0}{kr} \frac{[Q_\nu^m(\cos \theta_2)P_\nu^{m'}(\cos \theta_1) - P_\nu^m(\cos \theta_2)Q_\nu^{m'}(\cos \theta_1)]}{[Q_\nu^m(\cos \theta_2)P_\nu^m(\cos \theta_1) - P_\nu^m(\cos \theta_2)Q_\nu^m(\cos \theta_1)]} \quad (4)$$

where $Q_\nu^m(\cos \theta)$ is an associated Legendre function of the 2st kind of ν order. When $kr \gg 1$ at the aperture of a horn and $kb \ll 1$, it has shown that

$\nu \simeq kr$ and that the open-circuit condition ($Y=0$) is satisfied with $kr(\theta_2 - \theta_1) = \pi(l + \frac{1}{2})$. Thus, the slot depth is calculated as

$$d = r(\theta_2 - \theta_1) = \frac{\lambda}{4}(2l+1) \quad (5)$$

where l is integer and λ is wavelength in the corrugated conical horn.

In Fig. 1, provided that $b < \lambda/2$, only TM spherical mode exists within the corrugation and it can be proved $d = \lambda/4$ from the condition $E_\phi = 0$ at $\theta = \theta_1$. When corrugation depth is $\lambda/4$, Mantzer demonstrates that the beam pattern is most favorable in the condition $a = \lambda/8$ and $b/a = 0.75$. Mantzer's method for determining the corrugation width and separated ratio was utilized in this paper.

For balanced hybrid conditions, the particular case $Y=0$, the radiation pattern of the feed horn is circularly symmetric and the cross-polarization component is zero. When Y equals zero, equation (2) and (3) are reduced to

$$p_\nu^m(\theta_1)^2 = \frac{-m^2}{\sin^2 \theta_1} (h_\nu)^2 \quad (6)$$

$$\overline{A} = -p_\nu^m(\theta_1) \frac{\sin \theta_1}{m} = \pm 1 \quad (7)$$

When the ratio of electric-field and magnetic-field components is the same to the free space wave impedance, that is, $E_r/H_r = \pm j(\mu_0/\epsilon_0)^{1/2}$, we refer to this as the balanced hybrid condition. The positive sign corresponds to HE modes, the negative sign is to EH modes.

In balanced hybrid condition, the electric-field and magnetic-field at the horn aperture $P(\gamma, \theta, \phi)$ is

$$\begin{aligned}
 E_{\vartheta} &= -\eta_0 \frac{A \hat{H}_{\nu}}{\gamma} \left(\frac{P_{\nu}^1}{\sin \vartheta} + \frac{dP_{\nu}^1}{d\vartheta} \right) \cos \varphi \\
 E_{\varphi} &= \eta_0 \frac{A \hat{H}_{\nu}}{\gamma} \left(\frac{dP_{\nu}^1}{d\vartheta} + \frac{P_{\nu}^1}{\sin \vartheta} \right) \sin \varphi \\
 H_{\vartheta} &= -y_0 E_{\varphi} \quad , \quad H_{\varphi} = y_0 E_{\vartheta}
 \end{aligned} \quad (8)$$

The radiation field $\mathbf{E}(R, \theta, \phi)$ is determined from the aperture field over the range $P(\gamma, -\theta_1 < \vartheta < \theta_1, 0 < \varphi < 2\pi)$

$$\mathbf{E}(R, \theta, \phi) = \frac{jke^{-jkR}}{4\pi R} \mathbf{i}_R \times \int_S \{ \mathbf{i}_n \times \mathbf{E}_{\text{tan}} - \eta_0 (\mathbf{i}_n \times \mathbf{H}_{\text{tan}}) \} e^{jkr \mathbf{i}_n \cdot \mathbf{i}_s} ds \quad (9)$$

where \mathbf{i}_n , \mathbf{i}_R are unit vectors and the fields \mathbf{E}_{tan} , \mathbf{H}_{tan} are tangential components to the aperture of corrugated conical horn.

III. Shaped offset cassegrain antenna

Fig. 2 shows the cross section of the offset dual-reflector system for optimal design. The electric-field pattern propagating into the reflector is considered as Gaussian distribution.

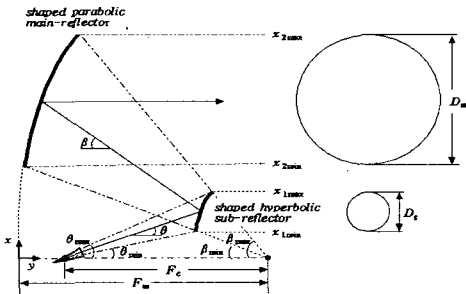


Fig. 2. Geometry of the shaped offset cassegrain antenna system

The power density is variable at an arbitrary point (x_2) of the main-reflector. In order to settle the problem, the conservation principle of energy was utilized. The principle is expressed as

$$\int_{\theta_{\min}}^{\theta_{\max}} E(\theta) 2\pi \sin \theta d\theta = \int_{x_{\min}}^{x_{\max}} I(x) 2\pi x dx \quad (10)$$

where the quantity $E(\theta)$ is the power density radiated from the corrugated conical horn as function of θ and $I(x)$ is the power density of the main-reflector. $I(x)$ must be a constant to have the uniform power density at the aperture of the main-reflector, and the curvature of the sub-reflector must satisfy Snell's law. θ_{\max} and θ_{\min} are the radiating angle toward the upper edge and lower edge of the sub-reflector. x_{\max} and x_{\min} are the maximum value and minimum value of x-axis of main-reflector or sub-reflector.

Normalizing by the total power, and performing the integration with the respect to x , these are represented as follows:

$$x = x_{\max} \left[\frac{\int_{\theta_{\min}}^{\theta} E(\theta) \sin \theta d\theta}{\int_{\theta_{\min}}^{\theta_{\max}} E(\theta) \sin \theta d\theta} \right]^{\frac{1}{2}} \quad (11)$$

$$\cos \beta = \cos \beta_{\min} - \left[\cos \beta_{\min} - \cos \beta_{\max} \right] \frac{\int_{\theta_{\min}}^{\theta} E(\theta) \sin \theta d\theta}{\int_{\theta_{\min}}^{\theta_{\max}} E(\theta) \sin \theta d\theta} \quad (12)$$

where β_{\max} and β_{\min} are the radiating angle toward the upper edge and lower edge of the main-reflector. The application of Snell's law to the perfectly conducting reflector surfaces defines a relationship between the angles shown and the slopes of it.

$$\frac{1}{r} \frac{dr}{d\theta} = \tan\left(\frac{\theta + \beta}{2}\right) \quad (13)$$

$$-\frac{dy}{dx} = \tan\left(\frac{\beta}{2}\right) \quad (14)$$

Equations (10)~(14) are sufficient to specify completely the reflector contour for a given reflector diameter. The curvature coordinates of the reflector satisfying the condition of uniform phase at the aperture can be obtained.

In the antenna with aperture, the efficiencies are calculated with the aperture. The analysis of efficiencies is very important. There are various kinds of efficiencies. If the shaped offset cassegrain antenna system combined with the corrugated conical horn has in phase and uniform amplitude, the important efficiencies determining antenna size and gain are the spillover (η_s) and the illumination (η_i). The total efficiency of the antenna system can be obtained by multiplying two efficiencies. These efficiencies and antenna gain are defined as follows:

$$\eta_s = \frac{\int_{\theta_{\min}}^{\theta_{\max}} E^2(\theta) \sin \theta d\theta}{\int_0^{\pi} E^2(\theta) \sin \theta d\theta}$$

$$\eta_i = 2 \cot^2\left(\frac{\theta_{\max}}{2}\right) \frac{\left| \int_{\theta_{\min}}^{\theta_{\max}} E(\theta) \tan\left(\frac{\theta}{2}\right) d\theta \right|^2}{\int_0^{\pi} |E(\theta)|^2 \sin(\theta) d\theta}$$

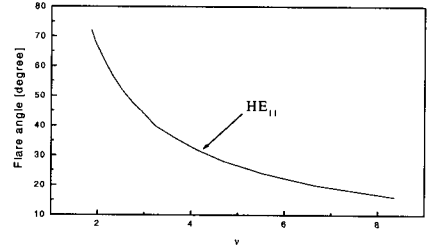
$$G = \left(\frac{\pi D_m}{\lambda}\right)^2 \eta_s \eta_i \quad (15)$$

where G is a system gain of the shaped offset cassegrain antenna and D_m is the diameter of the main reflector.

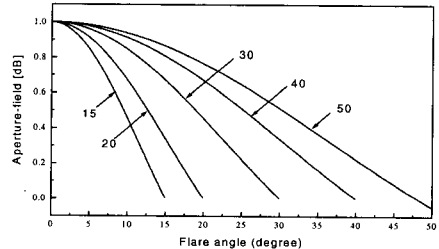
IV. Design and investigation of the shaped offset cassegrain antenna

4.1 Aperture field pattern and design of the corrugated conical horn

The aperture field pattern of the corrugated conical horn can be calculated using (8)~(9). The patterns are dependent on the flare angle and horn length, and are used to calculate the spillover and the illumination efficiency. Fig. 3 shows the flare angles of conical horn according to the order ν values and aperture field distribution of the conical horn. If the flare angle has 20° in Fig. 3, the order ν value will be equated to 6.43.

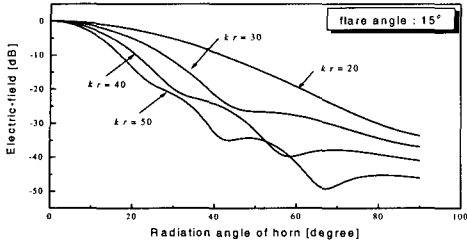


(a)

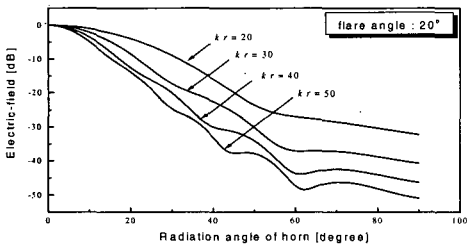


(b)

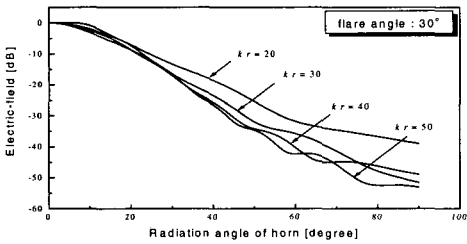
Fig. 3. (a) The ν characteristic curve on HE_{11} mode according to flare angles
(b) Normalized aperture-field distribution for corrugated conical horn



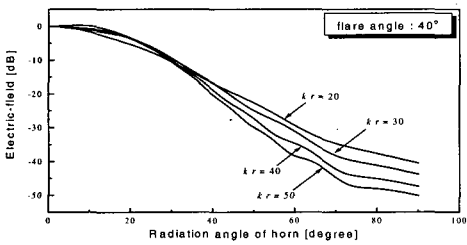
(a)



(b)



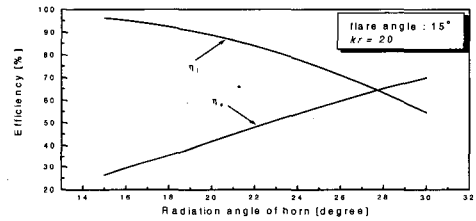
(c)



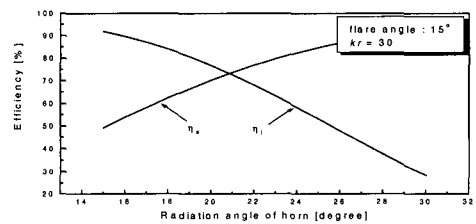
(d)

Fig. 4. Radiation pattern for corrugated conical horn with flare angle ($\theta_1=15^\circ, 20^\circ, 30^\circ, 40^\circ$)

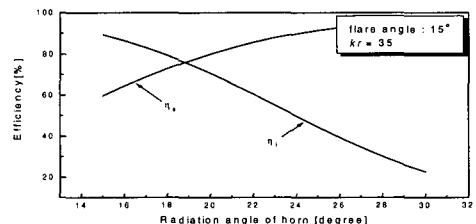
When the flare angle have some degrees, Fig. 4 shows the radiation patterns and characteristics according to the horn length(kr). we can find that should be the larger horn length and its flare angle between 15° and 30° . But radiation pattern is to be broad as soon as the flare angle has over 30° . In case horn length is fixed to the constant value, when radiation pattern has quickly declination, spillover efficiency is larger and illumination efficiency is smaller. Also, total efficiency has maximum value at the across point of illumination and spillover efficiency. Therefore, if we want to design the corrugated conical horn antenna with better efficiency, we should select the flare angle between 15° and 30° and the larger horn length.



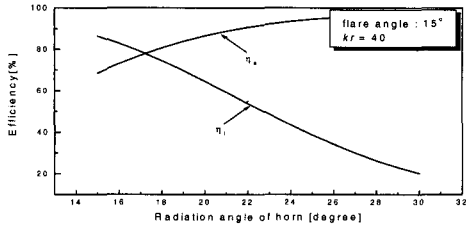
(a)



(b)



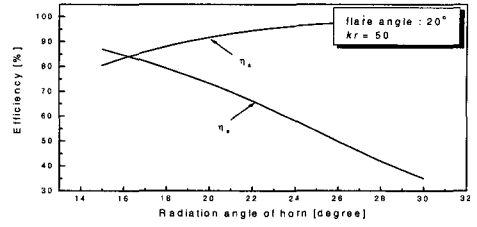
(c)



(d)

Fig. 5. Illumination and spillover efficiency for flare angle 15°

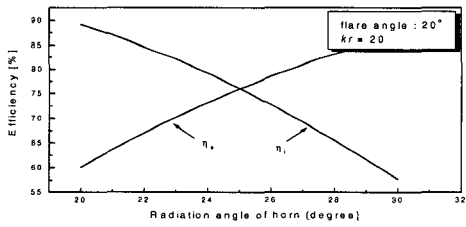
- a) $k\gamma = 20$, b) $k\gamma = 30$,
c) $k\gamma = 35$, d) $k\gamma = 40$



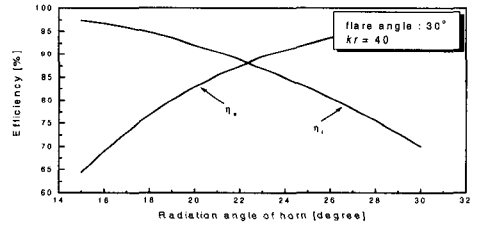
(d)

Fig. 6. Illumination and spillover efficiency for flare angle 20°

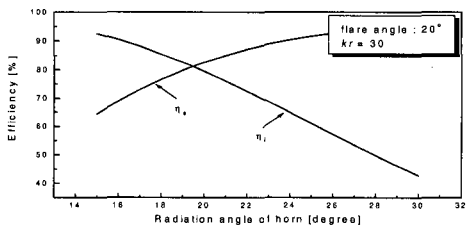
- a) $k\gamma = 20$, b) $k\gamma = 30$,
c) $k\gamma = 35$, d) $k\gamma = 40$



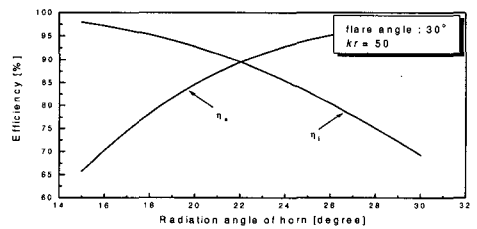
(a)



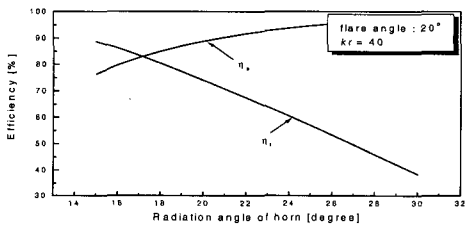
(a)



(b)



(b)



(c)

Fig. 7. Illumination and spillover efficiency for flare angle 20°

- a) $k\gamma = 40$, b) $k\gamma = 50$

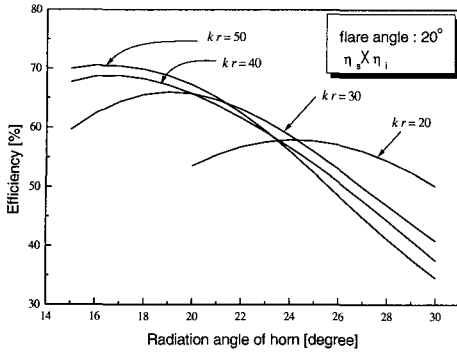


Fig. 8. Total efficiency($\eta_s \times \eta_i$) characteristic curves for flare angle 20°

When total efficiency($\eta_s \times \eta_i$) is the largest, the design data of the flare angle and the horn length($k\gamma$) can be realized. At this time, if we consider the total efficiency and reflector size, the design data must be determined in the range $\theta_1(\text{flare angle}) \leq 20^\circ$, $15 \leq k\gamma \leq 50$. From Fig. 3(b)~Fig. 8, when the design data of the corrugated horn which are $\theta_1 = 20^\circ$, $k\gamma = 50$ and $\theta = 16^\circ$, total efficiency is most favorable as 70.5 percentage.

Fig. 9 shows the designed corrugated conical horn operating at Ka-band frequency(21/30GHz) with $\theta_1 = 20$. The designed data of tooth duration width (a), slot width(b) and slot depth(d) are 1.79mm, 1.34mm and 3.57mm, respectively.

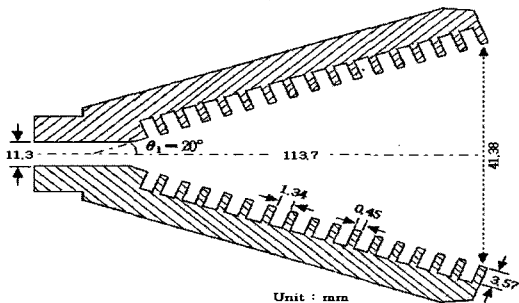


Fig. 9 Designed corrugated conical horn

4.2 Design of the shaped offset cassegrain antenna

In order to design the main and sub-reflector, the parameters θ_1 , θ_{\max} are primarily determined and the real size of reflector is determined by focus length.

Fig. 10 shows the shaped offset cassegrain antenna system operating in Ka-band frequency which is determined with 44cm focus length. It illustrates the direction of the reflected waves at each reflector. The corrugated conical feed horn lay in bottom of main-reflector to minimize the reflecting energy at the sub-reflector. In Table 1~2, the design data of cassegrain antenna and profiles are presented.

Table 1. The designed parameters and the calculated characteristics

Title	Method	Proposed method	SABOR method
Design parameters	D_m (cm)	58.16	58.16
	D_s (cm)	8.33	8.33
	F_c (cm)	44	44
	F_m (cm)	54	54
	θ_{\max} (deg.)	27.3	27.3
	θ_{\min} (deg.)	3.7	3.7
	β_{\min} (deg.)	3.78	3.78
Calculated characteristics	illumination(η_i)	84.61%	83%
	spillover(η_s)	83.33%	60%
	total efficiency ($\eta_i \times \eta_s$)	70.5%	49.8%
	antenna gain[dB]	40.5	39.1

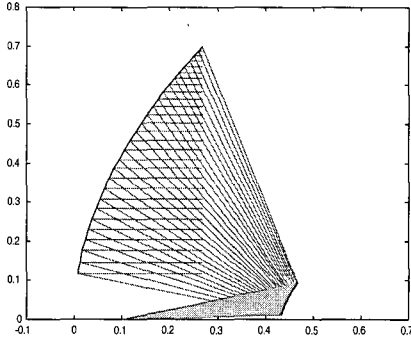


Fig. 10. Shaped offset cassegrain antenna system with focus length ($F_c = 44\text{ cm}$)

Table 2. Profiles for the curvature of main-reflector and sub-reflector

Sub-reflector		Main-reflector	
$x_1(\text{cm})$	$y_1(\text{cm})$	$x_2(\text{cm})$	$y_2(\text{cm})$
1.14	0.08	11.74	0.78
1.41	0.12	14.64	1.21
1.68	0.16	17.52	1.73
1.95	0.22	20.37	2.33
2.23	0.28	22.88	2.94
2.50	0.34	25.68	3.70
2.78	0.42	28.43	4.52
3.06	0.49	30.84	5.32
3.34	0.58	33.51	6.27
3.63	0.67	36.14	7.29
3.92	0.77	38.70	8.35
4.21	0.88	40.94	9.34
4.51	0.99	43.39	10.48
4.80	1.11	45.78	11.66
5.11	1.24	48.11	12.86
5.41	1.37	50.11	13.94
5.72	1.50	52.29	15.16
6.04	1.65	54.39	16.39
6.36	1.80	56.19	17.48
6.68	1.95	58.13	18.69
7.01	2.11	59.98	19.88
7.35	2.28	61.74	21.04
7.69	2.44	63.22	22.04
8.03	2.62	64.79	23.13
8.38	2.80	66.26	24.17
8.74	2.98	67.63	25.15
9.10	3.17	68.75	25.96
9.47	3.36	69.90	26.82

In Fig. 10, it can be shown that the wave direction passing through the aperture of the main-reflector is horizontal. It's clear that it satisfies the condition of total reflection based on Snell's law. Using this method of design, we can determine the design of the shaped offset cassegrain antenna having desired size and gain as controlled by the focus length. From the calculated efficiencies and the designed size of the main-reflector, power gain of the shaped offset cassegrain antenna system has been obtained 40.5dB gain in Ka-band frequency(21/30GHz). It has better characteristics than the result of SABOR[7] having the same design parameters.

V. Conclusion

In this paper, we presented the design of the shaped offset cassegrain antenna system with corrugated feed horn which has been mainly used in antennae for satellite-communication earth stations.

Applying spherical-mode analysis, we led the electromagnetic formula inside the corrugated conical horn. The flare angle and the horn length were determined by efficiency investigation. Then, with the former data, we designed the Ka-band corrugated conical horn. At the shaped offset cassegrain antenna system, the main and sub-reflector were designed using Snell's law and the conservation principle of energy: that is, the curvature of the main-reflector was calculated from the conservation principle of energy which means that the feed energy of the horn is uniformly distributed at the aperture. Then the curvature of the main-reflector was modified to have uniform path-length leading from feed point to the aperture.

The design procedure of shaped offset cassegrain antenna system presented in this paper can be used in the antenna design for satellite-communication. Also we can design the antenna having desired size and gain as

controlled by the flare angle of the horn and the focus length.

References

- [1]. P. J. B. Clarricoats and P. K. Saha, "Propagation and Radiation Behaviour of Corrugated Feeds", Part 2, Proc. Inst. Elec. Eng., vol. 118, pp. 1177 - 1186, Sept. 1971.
- [2]. J. K. M Jansen, M. E. J. Jeuken and C. W. Lambrechtse, "The Scalar Feed", Arch. Elek. Ubertragung., vol. 26, pp. 22-30, Jan. 1972.
- [3]. C. A. Mentzer, "Properties of Cutoff Corrugated Surfaces for Corrugated Horn Design", IEEE Trans. Antennas Propagat., vol. AP-22, pp. 191-196, 1974.
- [4]. P. W. Hannan, "Microwave Antenna Derived from the Cassegrain Telescope", IRE Trans. Antennas Propagat., vol. AP-9, pp. 140-153, Mar. 1961.
- [5]. G. W. Collins " Shaping of Subreflectors in Cassegrain Antenna for Maximum Aperture Efficiency", IEEE Trans. Antennas Propagat., vol. AP-21, pp. 309-313, May 1973.
- [6]. P. J. B. Clarricoats and A. D. Olver, *Corrugated Horns for Microwave Antennas*, IEE Electromagnetics Waves Series 18, Peter Peregrinus Ltd., pp. 58-96, 1984.
- [7]. M. a. Campo, F. J. del Ray, J. L. Besada and L. de Haro, " SABOR: Description of the methods applied for a Fast Analysis of Horn and Reflector antennas ", IEEE Antennas and Propagation Magazine, vol. 40, no. 4, pp. 95-107, Aug. 1998.

저 자 소 개



梁斗榮 (正會員)

1984년 2월 제주대학교 통신공학과 졸업(공학사). 1989년 2월 한양대학교 전자통신공학과 졸업(공학 석사). 1992년 2월 한양대학교 전자통신공학과 졸업(공학 박사).
1992년 3월 ~ 현재 제주대학교

통신공학과 부교수.

주관심 분야 : 안테나 및 전파전파, 마이크로파 및 RF 회로 설계, 위성·이동통신 시스템